Preliminary study on precursor information of loading and unloading failure of fractured sandstone in cold regions

Dongyang Han*, Yongjun Song, Huimin Yang

School of Architecture and Civil Engineering, Xi 'an University of Science and Technology, Xi 'an, Shaanxi, 710054, China

*Corresponding author's e-mail:hdy19149407 26@163.com

Abstract. The rock body engineering in the western cold region is prone to engineering geological disasters under the joint action of freezing, thawing and cyclic loading. In order to study the failure precursor information under the combined action of the two, the real-time acoustic emission (AE) monitoring test in the process of freeze-thaw fracture and complete white sandstone grading loading and unloading was carried out. The evolution characteristics of AE parameters of loaded rock were analyzed, and the AE precursor characteristics of rock instability were deeply explored. The results of the study show that the AE ringing counts of sandstones appear to have a relatively steady increase-surge period before destruction, and the appearance of the surge period signals the imminent rupture and failure of the rock; The acoustic emission *b*-value of the fissured sandstone decreases abruptly before destabilisation, and the failure is sudden; while the intact sandstone undergoes a short fluctuation after the sudden decrease, and the sudden decrease in *b*-value can be used as a precursor feature of destabilisation damage. The Felicity ratio decreases approximately linearly with the increase of loading and unloading grade, and the damage degree of sandstone increases continuously. The comprehensive analysis of AE ringing count, *b*-value and Felicity ratio can improve the reliability of sandstone instability prediction. The research results can provide reference for the analysis and prevention of rock mass engineering disasters in cold regions.

Keywords: Loading and unloading; Freeze-thaw cycles; Acoustic emission *b*-value; Failure precursors.

1 Introduction

With the construction of large-scale projects such as transport, hydropower and other large-scale projects in the western region of China, the related rock projects are more and more frequently encountered with a variety of geological hazards (earthquakes, landslides, landslides, etc.) and engineering disasters (rock bursts, collapses, rock instability, etc.) [1-2], which cause huge economic losses. The macro-disaster of rock body originates from the gradual expansion of local damage, and this process contains

P. Liu et al. (eds.), *Proceedings of the 2024 5th International Conference on Civil, Architecture and Disaster Prevention and Control (CADPC 2024)*, Atlantis Highlights in Engineering 31,
https://doi.org/10.2991/978-94-6463-435-8_39

rich precursor information, and its prediction and forecasting have important engineering value for disaster prevention and control.

In fact, engineering rock bodies are often subjected to cyclic loading, such as excavation and support of slopes, transport loads, etc. [3]. Its essence is the increase and release of stresses on the rock body, internal cracks sprouting, expansion, aggregation and penetration, resulting in damage and gradual accumulation, leading to premature failure and destruction of the rock body, thus inducing engineering disasters [4]. Since rocks under cyclic loading show different mechanical properties from those of conventional tests, some scholars have explored the deformation damage and damage evolution law of rocks during cyclic loading and unloading [5-8]. In addition, the water in the pores of the rock body in the cold region causes damage to the rock during repeated freezing and thawing [9], thus weakening the mechanical properties and stability of the rock body [10], leading to a significant increase in the risk of geological disasters. At the same time, the presence of fissures in the natural rock mass significantly reduces the strength and deformation resistance of the rock mass [11]. Compared with the small defects inside the rock mass, the volume expansion of water in larger defects such as fissures produces frost concentration around the fissures, and the local damage is more serious [12]. Therefore, for rock engineering in cold regions, the fatigue damage caused by cyclic loading should not be neglected, and compared with only considering the freeze-thaw damage effect, the mechanical properties of the rock body are greatly weakened under the joint action of freeze-thaw and cyclic loading [13], which seriously threatens the safety and stability of the rock body. People have done a lot of research on the fatigue mechanical behaviour of freeze-thaw rocks under loading and unloading [14], energy dissipation [15], fracture mechanism [16], and damage evolution characteristics [17], and achieved remarkable results. Some scholars have studied the damage characteristics and failure mechanism of rock under loading and unloading based on acoustic emission detection technology [18-20].However, there are few reports on the failure precursor characteristics of frozen-thawed rock under cyclic loading.

In summary, the current research on freeze-thaw rock loading and unloading failure mainly focuses on mechanics and damage mechanism, and there is little research on the precursor information of freeze-thaw rock loading and unloading failure. Therefore, in this paper, real-time acoustic emission monitoring tests of graded loading and unloading are carried out on cracks and intact white sandstone after different freeze-thaw cycles. The acoustic emission characteristics of the whole process of rock loading and unloading fracture evolution are analyzed, and the precursor characteristics of rock instability acoustic emission are deeply explored in order to improve the accuracy of instability prediction.

2 Pilot programme

2.1 Preparation of rock samples

The original rock is taken from a rocky slope in the cold western region of China, and its main components are quartz, potassium feldspar, kaolinite and illite. The problem of short intermittent joints is widespread in rock engineering, and rocky slopes

containing one or more sets of slow-steep inclination intermittent joints are prone to destabilisation and slippage under gravity or applied loads and thus form step-path damage [21]. The strength of the rock mass reaches its minimum when the connectivity of the joints is small and the dip angles are 30° and 60° [22]. Therefore, 30° and 60° were used to represent slow and steep inclination joints, respectively, and the penetration degree of the prefabricated fissure of the specimen was set to be 20%, and its lengths were calculated to be 20 mm and 12 mm, respectively. The height of the rock bridge area and inclination angle were set to be 15 mm and 90°, respectively. According to the test protocol of the International Society of Rock Mechanics, the core taken from the borehole was from the same original rock, and the core was cut and processed into a standard cylindrical rock sample of Φ50mm×H100mm, with the degree of non-parallelism of the two end surfaces less than 0.05mm, and the sandstone with obvious differences in appearance was rejected. As shown in Figure 1.

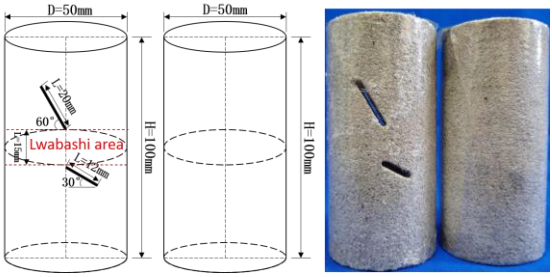

Fig. 1. Examples of rock samples.

The drilled and polished sandstones were put into the oven and dried at a constant temperature of 105°C for 48 h. After the sandstones were cooled down, the dry density and longitudinal wave velocity were measured, and then put into the vacuum saturator to saturate the sandstones for 24 h and measure the porosity. According to the principle of similarity of physical parameters, 18 intact and fissured sandstones were selected respectively. The average physical parameters of the sandstones are shown in Table 1.

Table 1. Average physical parameters of sandstone

Test piece	Dry density($g \cdot cm^{-3}$)	Porosity(%)	Wave velocity($m \cdot s^{-1}$)
Fractured rock	2.25	11.12	2201
Intact rock	2.31	10.71	2278

The selected fissured and intact sandstones were divided into three groups of six each and placed into a low-temperature freeze-thaw cycling chamber for freeze-thaw tests after the sandstones were fully saturated. The rocky slope is located in a region where the lowest average temperature in some months can reach about -20°C. With reference to the specification of ISRM Recommended Methods for Rock Characterisation, Testing and Monitoring: 2007-2014, the freezing temperature was set at -20°C and the thawing temperature at 20°C, which lasted for 12h and 24h as a freeze-thaw cycle, respectively. The number of freeze-thaw cycles for each group of the two sandstones was set to 0, 15 and 30 cycles, respectively, according to the temperature variations in

the cold region, in order to simulate the damage caused to the rocks by different freeze-thaw cycles.

2.2 Real-time acoustic emission test with graded loading and unloading

At the end of the freeze-thaw cycle test, three sandstones from each group were taken for uniaxial compression to obtain the compressive strength and the average value was calculated. As shown in Table 2.

Table 2. Sandstone grouping number and average compressive strength

Number of freezing and thawing	0 Times	15 Times	30 Times
Fractured rock	F-0	F-15	F-30
Average compressive strength(MPa)	11.85	8.77	5.90
Intact rock	C-0	C-15	C-30
Average compressive strength(MPa)	25.02	19.78	14.18

The graded loading and unloading stress levels of the remaining sandstone were set to 50%, 60%, 70%, 80% and 90% of the average compressive strength, and the last level was loaded until destruction. The test was stress-controlled, and the loading and unloading rates were 0.02 MPa/s. The acoustic emission system was debugged before the start of the test, the acoustic emission threshold was set to 40 dB, the sampling frequency was 2 MHz, and the acoustic emission transducer was tightly affixed to the surface of the sandstone using the coupling agent. The rock mechanics testing machine and the acoustic emission system are shown in Figure 2. Limited to space, this paper takes one representative rock sample from each group of specimens to analyse the results.

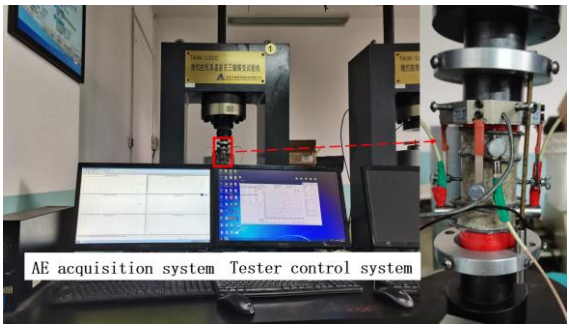

Fig. 2. Test system

3 Test results and analyses

3.1 Acoustic Emission Ringer Counting Characteristics

During cyclic loading and unloading, the rock is accompanied by the compaction of primary defects and the emergence, expansion, aggregation and penetration of new-

born cracks, and the AE ringing counts can reflect the degree of internal damage in the rock in real time. Figure 3 shows the variation curve of time-stress-ringer counts under graded loading and unloading.

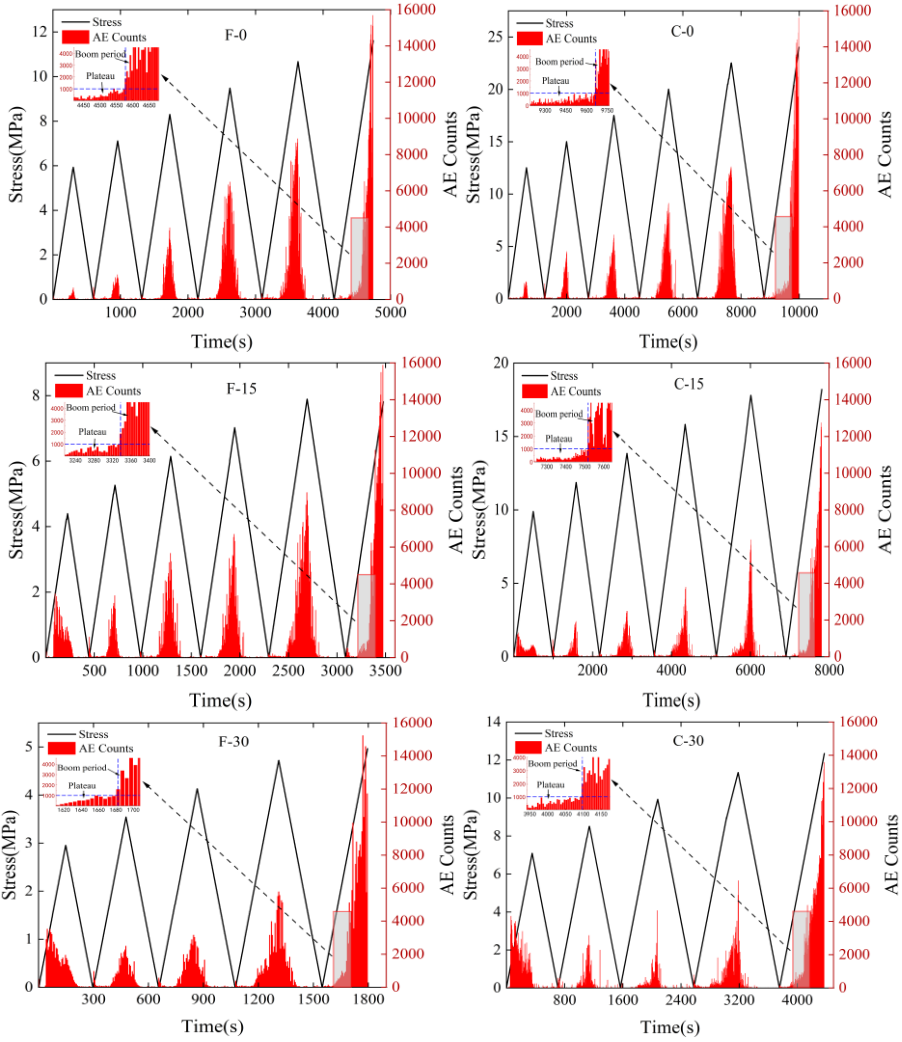

Fig. 3. Time-stress-ringer count relationships for fractured and intact sandstones at different freeze-thaw counts

First loading and unloading: fissured and intact sandstones have similar trends in ringer counts. That is, as the number of freezing and thawing increased, the overall ringing counts increased at the beginning of loading. The peak ringing counts of the two sandstones without freezing and thawing appeared at the stress peak, and the sandstones after freezing and thawing moved forward from the stress peak and reached the maximum value at the stress of about 1~2 MPa. This is due to the sandstone in the

process of freeze-thaw cycle damage, resulting in local microfractures and microporosity and other defects, when the sandstone is applied to the axial stress of 1~2 MPa, that is, more than the cohesion between the particles and particles, these micro-defective structures quickly fracture and be compacted, the instantaneous release of a large amount of energy and elasticity of the wave, resulting in the counts of the surge and reach the peak, and then the sandstone as a whole is to be continued to be compacted, the ring counts are also gradually reduced. The ringing counts gradually decreased. During unloading, a small number of AE ringing counts were generated due to the elongation of a small number of microcracks.

Intermediate levels of loading and unloading (2nd-5th or 2nd-4th loading and unloading): The pattern of variation of ringing counts is similar for each level of loading and unloading. After the first unloading, the micro-defects are compacted, making the sandstone internal whole tends to be complete, the two sandstones in the early stage of each loading acoustic emission period, almost no acoustic emission counts generated. As loading continues, microcracks continue to develop in the sandstone, and the AE ringing counts begin to increase, reaching a maximum value at the peak stress of each unloading stage, while the crack development is also the most intense.

The final loading failure stage: When it is close to the peak stress, a large number of microcracks expand, and the surface cracks and internal cracks of sandstone intersect to form macroscopic cracks. The AE ringing count increases sharply, indicating that the rock sample will break and fail in a short time. All sandstone ringing counts have this change characteristic. As shown in the enlarged area in Figure 3, before the sandstone damage, the AE ringing counts showed a period of relatively steady increase, at this time, the internal microcracks in the sandstone continued to develop stably. According to the variation of ringing counts, the counts fluctuate and increase in the range of 100 to 1000, with a short-term surge when the counts exceed 1000, followed by sandstone destabilisation and damage. Therefore, the time period of 100 to 1000 counts is regarded as a period of relative steady increase of AE, and its percentage is calculated as:

$$P = \frac{t_i}{t_j} \times 100\% \tag{1}$$

Where: t_i is the length of the relative stabilisation period, and t_j is the length of the period from the beginning of the relative stabilisation period to the destruction of the rock sample.

The relative steady increase period percentage is shown in Table 3. The percentage of relative steady increase period of two sandstones AE decreases with the increase of the number of freezing and thawing, which indicates that the more the number of freezing and thawing, the more serious the damage is, and most of the microcracks have already finished expanding before sandstone damage, and rapidly gather to form macroscopic cracks at the time of damage, whereas sandstones with less freezing and thawing have less degree of crack development before damage, and still need to continue to develop and produce more acoustic emission signals, so the percentage of relative steady increase period is relatively long. The increase in the number of freezing and thawing times decreases the steady increase period and prolongs the surge period in

sandstone, and combining the two phenomena at the same time will be more effective in predicting rock instability.

Table 3. Percentage of relatively stable growth period

Rock	F-0	F-15	F-30	C-0	C-15	C-30
P(%)	52.72	43.19	33.47	57.98	47.03	39.96

3.2 The pattern of variation of acoustic emission b-value

The calculation of the *b*-value evolved from the development of the Gutenberg-Richter [23] magnitude-frequency relationship, which is expressed as:

$$LgN = \mathrm{a} - \mathrm{b}M \tag{2}$$

where N is the earthquake frequency, M is the earthquake magnitude, and a, b are constants. Instead of magnitude M, the amplitude is usually divided by 20 in the AE parameters, and instead of N,a is a constant and b is the *b*-value, the sum of the AE data in each time window, the formula becomes:

$$LgN = \mathrm{a} - b\frac{A_{db}}{20} \tag{3}$$

In this paper, the least squares method is used to calculate the acoustic emission *b*-value, which is usually used to describe the crack scale size and reflect the dynamic expansion of cracks in the loading process. As shown in Figure 4, the *b*-values of the two sandstones have a decreasing trend, and the small-scale cracks are continuously connecting and developing to the large-scale cracks. During the first unloading process, the *b*-value of the sandstone fluctuates up and down for 30 times of freezing and thawing, and the internal micro-defects are in an unstable state in the short-term compression and densification. During the loading and unloading of the intermediate series, the b-value fluctuates slightly, and the crack development is relatively stable during this process.

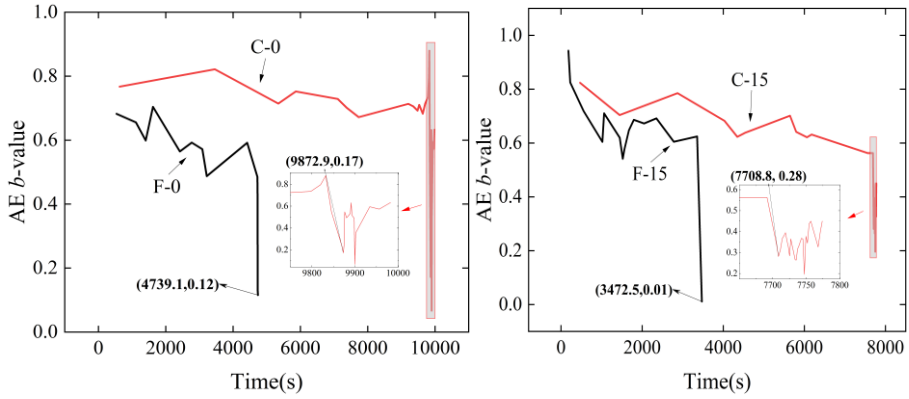

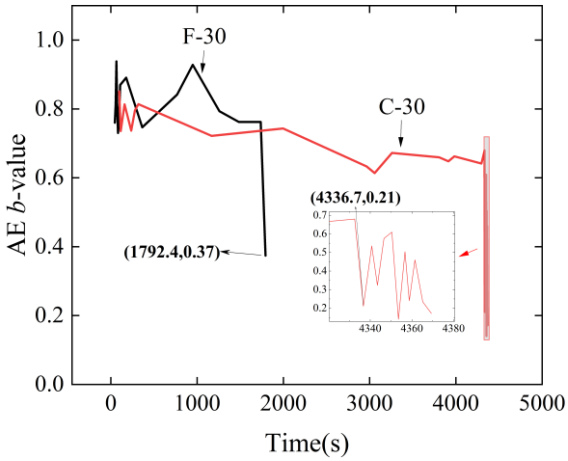

Fig. 4. The pattern of variation of acoustic emission *b*-value

In addition, the change pattern of *b*-value varies between the fissured and intact sandstones, which is mainly manifested in the last level of loading failure process. Before the destruction of fissured sandstone, the *b*-value decreases rapidly, and brittle destruction occurs from the rock bridge area to the cracks at both ends of the fissure, as shown in Figure 5(a). It is shown that the rock crack development is extremely unstable at this stage, and the cracks penetrate each other before failure, forming larger scale macrocracks close to the peak stress, which leads to a sudden drop in the acoustic emission *b*-value. The *b*-value of intact sandstone decreases and then rises slightly before failure, and there is a section of obvious up and down fluctuation area. The crack development also shows an unstable state, and finally a macroscopic through crack is produced, as shown in Figure 5(b). It can be seen that a significant decline in *b*-value indicates that the sandstone is about to be damaged, with the first plunge in *b*-value as the precursor point, corresponding to the size and time of the value as shown in Table 4. Because of the similarity of *b*-value rule of the same sandstone, take the unfrozen and thawed sandstone as an example. *b*-value drops from 0.49 to 0.12 before F-0 failure, and the damage occurs after 4 s. *b*-value drops from 0.55 to 0.17 before C-0 failure, and the sandstone becomes unstable after 117 s. The *b*-value drops from 0.55 to 0.17 before the failure. And combined with Table 4, it can be seen that the time difference from the appearance of precursor point to the destruction of fissured sandstone is extremely short, easy to sudden instability, and the destruction is more difficult to predict; while the intact sandstone undergoes short-term fluctuation before destruction, and the time difference under the same number of freezing and thawing times is about 7.8-31.0 times of that of fissured sandstone, with better precursor predictability.

Table 4. Acoustic emission *b*-value and precursor time

Rock	*b*-value	Precursor time(s)	Breaking time(s)	Time difference(s)
F-0	0.12	4739.1	4742.9	3.8
F-15	0.01	3472.5	3477.2	4.7
F-30	0.37	1792.4	1796.7	4.3
C-0	0.17	9872.9	9990.8	117.9
C-15	0.30	7708.8	7811.0	102.2
C-30	0.21	4336.7	4370.4	33.7

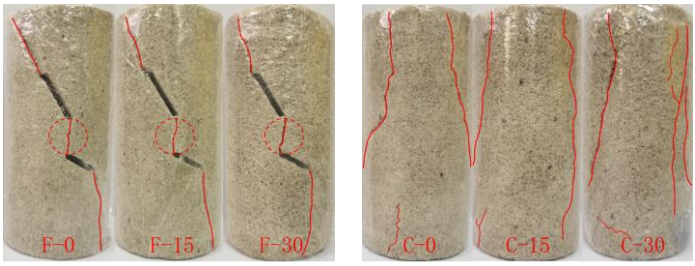

(a) (b)

Fig. 5. Distribution of damage cracks in sandstone

3.3 Loading and unloading Felicity effect

The Felicity Ratio is often used to test the accuracy of the memory properties of rock materials, with smaller ratios indicating that the acoustic emission memory is more advanced and the damage is more severe. It is generally believed that the ratio of 0.9 or more is accurate. Its calculation formula is:

$$F_i = \frac{\sigma_i}{\sigma_{i-1}} \tag{4}$$

Where: σ_i is the value of stress at the time of acoustic emission phenomenon in the ith cycle, and σ_{i-1} is the maximum stress value in the (i-1)th cycle.

At present, there is no uniform standard in defining the reappearance of acoustic emission phenomenon, according to the acoustic emission data changes in this test, the ringing count is defined as reappearance of acoustic emission phenomenon when it exceeds 100 for five times consecutively. As shown in Figure 6, the correlation between loading and unloading level and F_i shows that F_i decreases linearly with the increase of loading and unloading level, and the F_i of C-0 and F-0 in the second level of loading and unloading is above 0.9, which indicates that they have micro-defects after the first loading and unloading, and the memory characteristics of the rock samples at this time are more accurate, and the micro-defects of C-15 and F-15 are generated by the freezing and thawing cycle, and the F_i in the second level of unloading and unloading is below 0.83, and the memory characteristics of rock samples are ahead of the time. below, and the memory characteristics of the rock samples are ahead. The F_i of the same rock samples decreases with the increase of the number of freeze-thaw cycles, and all of them

are below 0.73 at 30 freeze-thaw cycles. With the increase of loading and unloading levels, the fatigue damage inside the same rock samples is also intensified, the irreversible deformation gradually increases, F_i decreases approximately linearly, and the memory characteristics of the rock samples are also gradually superprioritised. In the final loading stage of destruction, F_i drops to the minimum value, in the range of 0.27 to 0.41, and the same rock samples freeze and thaw for 30 times F_i is the smallest, the most serious degree of damage, this stage of the rock samples gradually close to the destruction. When F_i decreases gradually, the irreversible damage inside the rock samples accumulates gradually, and F_i decreases from the second stage of loading and unloading to the final loading damage by more than 51%. Freezing and thawing cycles and loading/unloading are the main factors leading to rock damage, and F_i can reflect the degree of damage caused by both of them, so the combination of Felicity ratio to predict the failure of freezing and thawing rocks can improve the accuracy.

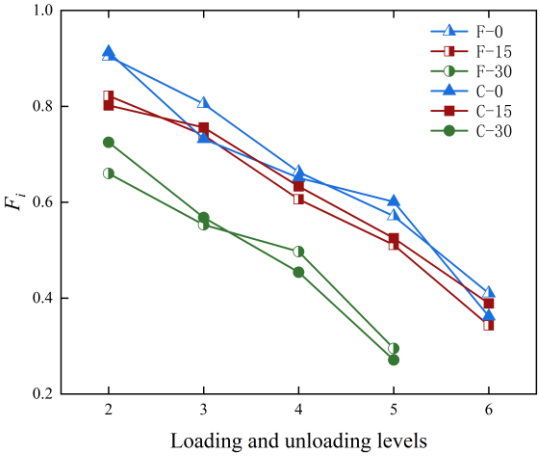

Fig. 6. The change curve of Felicity ratio under graded loading and unloading

4 Conclusion

In this paper, graded cyclic loading and unloading tests were carried out on freeze-thaw cracks and intact sandstone, and the acoustic emission precursor characteristics of freeze-thaw white sandstone failure under cyclic loading were studied. The main conclusions are as follows:

(1) The increase in the number of freezing and thawing events increased the damage level of the sandstone, which led to an overall significant increase in the number of ringing counts for the first loading and unloading events. Before approaching damage, the ringer counts went through a phase of relative steady increase-steep increase, with the proportion of relative steady increase decreasing with the increase of the number of freezing and thawing, and the appearance of the surge phase signalling the development of sandstone to the unstable state.

(2) Acoustic emission *b*-values generally tend to decrease with increasing loading level, and crack scales are expanding. Fractured sandstones show a sharp decrease in

b-value before failure, which makes failure more rapid and destabilisation prediction more difficult, while intact sandstones show a short fluctuation in *b*-value after a sharp decrease, which makes failure more moderate. When the *b*-value drops sharply, we should be alert to the instability and failure of sandstone.

(3) Freeze-thawed sandstone produces the Felicity effect, with acoustic emission memory properties overshooting. The Felicity ratio is negatively correlated with the number of freeze-thaw cycles, and decreases approximately linearly with the increase of loading grade, and the damage of sandstone is gradually aggravated. This ratio can reflect the damage of sandstone caused by freeze-thaw cycles and loading and unloading at the same time.

The destruction of freeze-thawed rocks by cyclic loading is a complex process, and acoustic emission monitoring can reflect the state of internal defects in rocks in real time, which is a powerful means to study the damage mechanism and failure precursors of rock materials. However, the use of a single means of research has certain limitations, and the indicators are relatively single. In future research, we can combine real-time CT scanning and infrared radiation with other technologies to study the microscopic and macroscopic characteristics of the damage precursors of rock loading and unloading, so as to reveal the damage mechanism from different perspectives and explore the characteristics of the damage precursors in depth.

Acknowledgments

This paper is one of the milestone results of the National Natural Science Foundation of China (Research on Damage Mechanism and Modelling of Jointed Rock Body under the Coupling of Freezing, Thawing and Long-term Load).

References

1. Xie, L.L., Qu, Z. (2018) On civil engineering disasters and their mitigation[J]. Earthquake Engineering and Engineering Vibration., 17: 1-10.
2. Xiao, P., Liu, H.X., Zao, G.Y. (2023) Characteristics of Ground Pressure Disaster and Rockburst Proneness in Deep Gold Mine[J]. Lithosphere., 2022(Special 11): 9329667.
3. Song, Z.Y., Konietzky, H., Wu, Y.F., et al. (2022) Mechanical behaviour of medium-grained sandstones exposed to differential cyclic loading with distinct loading and unloading rates[J]. Journal of Rock Mechanics and Geotechnical Engineering., 14(6): 1849-1871.
4. Yu, Y., Wang, Z.H., Wang, J., et al. (2022) Study on acoustic emission characteristics of granite under incremental repeated loading and unloading[J].Journal of Beijing Jiaotong University., 46(06):123-131.
5. Momeni, A., Karakus, M., Khanlari, G.R., et al. (2015) Effects of cyclic loading on the mechanical properties of a granite[J]. International Journal of Rock Mechanics and Mining Sciences., 77: 89-96.
6. Jing, L.W., Li, X.S., Yan, Y., et al. (2022) Study on constitutive model of coal rock damage under graded cyclic loading and unloading[J] Safety in Coal Mines., 53(01):71-78.

7. Miao, S.J., Liu, Z.J., Zhao, X.G., et al. (2021) Energy dissipation and damage characteristics of Beishan granite under cyclic loading and unloading[J]. Chinese Journal of Rock Mechanics and Engineering., 40(05):928-938.
8. Yang, K., Zhang, Z.N., Chi, X.L., et al. (2022) Experimental study on crack evolution and damage characteristics of water bearing sandstone under cyclic loading[J]. Rock and Soil Mechanics., 43(07):1791-1802.
9. Liu, Q.S., Huang, S.B., Kang, Y.S., et al. (2016) Study of unfrozen water content and frost heave model for saturated rock under low temperature[J]. Chinese Journal of Rock Mechanics and Engineering., 35(10):2000-2012.
10. Jia, H.L., Xiang, W., Krautblatter, M. (2015) Quantifying rock fatigue and decreasing compressive and tensile strength after repeated freeze-thaw cycles[J]. Permafrost and Periglacial processes., 26(4): 368-377.
11. Wu, J.Y., Feng, M.M., Yu, B.Y., et al. (2018) The length of pre-existing fissures effects on the mechanical properties of cracked red sandstone and strength design in engineering[J]. Ultrasonics., 82: 188-199.
12. Qiao, G.W., Wang, Y.S., Chu, F., et al. (2015) Failure mechanism of slope rock mass due to freeze-thaw weathering[J]. Journal of Engineering Geology., 23(03):469-476.
13. Shen, Y.J., Yang, H.W., Jin, L., et al. (2019) Fatigue deformation and energy change of single-joint sandstone after freeze-thaw cycles and cyclic loadings[J]. Frontiers in Earth Science., 7: 333.
14. Zhang, Q., Liu, Y., Dai, F., et al. (2022) Experimental assessment on the fatigue mechanical properties and fracturing mechanism of sandstone exposed to freeze-thaw treatment and cyclic uniaxial compression[J]. Engineering Geology., 306: 106724.
15. Shi, Z.M., Li, J.T., Wang, J. (2023) Energy Evolution and Fracture Behavior of Sandstone Under the Coupling Action of Freeze–Thaw Cycles and Fatigue Load[J]. Rock Mechanics and Rock Engineering., 56(2): 1321-1341.
16. Wang, Y., Han, J.Q., Li, C.H. (2020) Acoustic emission and CT investigation on fracture evolution of granite containing two flaws subjected to freeze–thaw and cyclic uniaxial increasing-amplitude loading conditions[J]. Construction and Building Materials., 260: 119769.
17. Wang, Y., Gao, S.H., Li, C.H., et al. (2021) Energy dissipation and damage evolution for dynamic fracture of marble subjected to freeze-thaw and multiple level compressive fatigue loading[J]. International journal of fatigue., 142: 105927.
18. Li, D.X., Wang, E.Y., Kong, X.G., et al. (2019) Damage precursor of construction rocks under uniaxial cyclic loading tests analyzed by acoustic emission[J]. Construction and Building Materials., 206: 169-178.
19. Meng, Q.B., Zhang, M.W., Han, L.J., et al. (2016) Effects of acoustic emission and energy evolution of rock specimens under the uniaxial cyclic loading and unloading compression[J]. Rock Mechanics and Rock Engineering., 49: 3873-3886.
20. Zhang, M.W., Meng, Q.B., Liu, S.D., et al. (2018) Impacts of cyclic loading and unloading rates on acoustic emission evolution and felicity effect of instable rock mass[J]. Advances in Materials Science and Engineering., 2018.
21. Huang, D., Cen, D.F., Ma, G.W., et al. (2015) Step-path failure of rock slopes with intermittent joints[J]. Landslides., 12: 911-926.
22. Chen, X., Liao, Z.H., Li, D.J. (2011) Experimental study of effects of joint inclination angle and connectivity rate on strength and deformation properties of rock masses under uniaxial compression[J]. Chinese Journal of Rock Mechanics and Engineering., 30(04):781-789.
23. Gutenberg, B., Richter, C.F. (1944) Frequency of earthquakes in California[J]. Bulletin of the Seismological society of America., 34(4): 185-188.